

# First-Principles Study of 30H-BN Polytypes

Kazuaki Kobayashi and Shojiro Komatsu

National Institute for Materials Science, Tsukuba 305-0044, Japan

We calculated the electronic and lattice properties of 30H-BN which are  $sp^3$ -bonded compounds. The 30H polytype has various over 6000000 structures. Their possible symmetries and hexagonalities ( $H[\%]$ ) are  $P6_3mc$  and  $P3m1$ , and 6.7%~93.3%, respectively. Hexagonality is a ratio of the number of hexagonal ( $h$ ) character and the total number of cubic ( $c$ ) and  $h$  characters in a unit cell. Two structures in the 30H polytype are considered in this study. Their stacking sequences (ABC notation) are ABCABCABCABCACBACBACBACB ( $P6_3mc$ ,  $H = 6.7\%$ ) and ABCBCBCBCBCBCBCBCBCBCBCB ( $P3m1$ ,  $H = 93.3\%$ ). Their lattice properties were optimized automatically by the total energy pseudopotential method. Calculated total energies of 30H-BN are in the order of ABCABCABCABCACBACBACBACBACBACB (6.7%) < ABCBCBCBCBCBCBCBCBCBCBCB (93.3%). Values in parentheses are hexagonalities (%). This means the former is energetically more favorable than the latter. The total energy of the BN polytype increases with increasing hexagonality. We calculated their electronic band structures, the band gap values, the valence band maximum (VBM), and conduction band minimum (CBM). Their electronic band structures are non-metallic and band gaps are indirect. [doi:10.2320/matertrans.MAW201004]

(Received April 23, 2010; Accepted May 24, 2010; Published August 25, 2010)

**Keywords:** 30H-BN, polytype, electronic band structure, first principles

## 1. Introduction

6H- and 30H-boron nitride (6H-BN, 30H-BN) are new materials that have been synthesized by Komatsu.<sup>1,2</sup> These polytypes<sup>3,4</sup> are  $sp^3$ -bonded compounds which consist of hexagonal cation and anion layers in a unit cell. Their possible symmetries are  $P6_3mc$  and  $P3m1$ .

The purpose of this study is to investigate the electronic and lattice properties of the 30H-BN polytype using the total energy pseudopotential method with the structure optimization and to compare with the experimental results.<sup>1</sup> The electronic properties are the electronic band structures, valence band maximum (VBM), conduction band minimum (CBM), band gap values, direct or indirect. Although there are many theoretical<sup>5-9</sup>) and experimental<sup>10</sup>) studies of BN compounds, there are no theoretical studies of 30H-BN. Furthermore, the electronic and structural properties of 30H-BN are not clear experimentally in detail<sup>1</sup>) with the exception of lattice constants. It is important to search wide band gap materials with the ultraviolet region ( $\sim 6$  eV). The electronic properties of synthesized 30H-BN are not clear although the minimum band gap values of BN<sup>10</sup>) are approximately 6 eV in experiment. It is expected that new usual properties will be obtained as a result of electronic structure calculations.

We have investigated the electronic and lattice properties of 2H~6H-BN (AlN, SiC)<sup>11,12</sup>) and 10H-BN (AlN),<sup>13</sup>) and 12H-BN.<sup>14</sup>) 2H~5H polytypes have unique structure, respectively. As for the 6H polytype, it has two structures as ABCACB and ABCBCB (ABC notation<sup>4</sup>). Figure 1 is the polytype structures of 6H-BN(ABCACB) and 6H-BN(ABCBCB). The polytype structure has cubic ( $c$ ) and hexagonal ( $h$ ) characters as shown in Fig. 1. Hexagonality is the ratio of the number of  $h$  character and the total number of  $c$  and  $h$  characters in the unit cell.<sup>12</sup>) 10H and 12H polytypes have 18 and 58 structures,<sup>15</sup>) respectively. In contrast, the 30H polytype has over 6000000 structures whose stacking sequences are different from each other,<sup>15</sup>) and possible crystal symmetries and hexagonalities ( $H[\%]$ ) are  $P6_3mc$  and  $P3m1$ , and 6.7%, 13.3%, 20%, 26.7%, 33.3%, 40%, 46.7%,

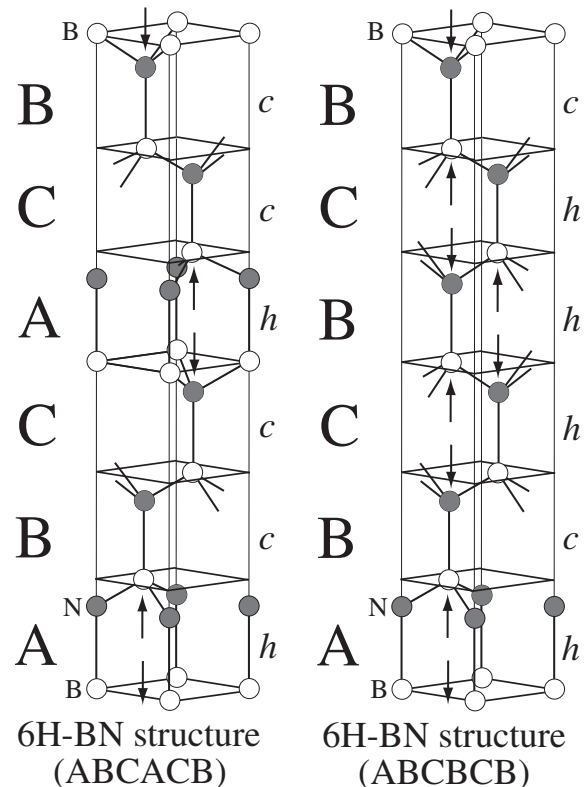


Fig. 1 Crystal structures of 6H-BN as ABCACB and ABCBCB. The cubic and hexagonal characters of the BN bilayers are indicated by “ $c$ ” and “ $h$ ”. The third-neighbor B-N atoms are indicated by arrows.

53.3%, 60%, 66.7%, 73.3%, 80%, 86.7%, and 93.3%, respectively. This number (6000000) is too huge to calculate all possible structures in the 30H polytype. Furthermore, the 30H polytype is three times as large as the 10H polytype<sup>13</sup>) and it is expected that the electronic structure calculations of 30H-BN need huge computer resources. In this study, we choose two stacking sequences as ABCABCABCABCACBACBACBACBACBACB and ABCBCBCBCBCBCBCBCBCBCBCB. Notations are the ABC notation. We

define hereafter “ABC—ACB” and “ABC—BCB” as shorter notations of ABCABCABCABCACBACBACBACBACB and ABCBCBCBCBCBCBCBCBCBCBCBCBCB, respectively. The symmetry and hexagonality ( $H$ [%]) of 30H-BN(ABC—ACB) are  $P6_3mc$  and 6.7% ( $\simeq 1/15$ ), and those of 30H-BN(ABC—BCB) are  $P3m1$  and 93.3% ( $\simeq 14/15$ ), respectively. One stacking sequence has smallest hexagonality (6.7%) and the other is largest hexagonality (93.3%) in the 30H polytype.

From the previous studies,<sup>12,13</sup> the total energies of BN and AlN polytypes have a relation to hexagonality ( $H$ ). This is an important parameter to discuss the stabilities of BN and AlN polytypes.<sup>12,13</sup> Energetical stabilities of BN and AlN polytypes are described by the number ( $N_{\text{third}}$ ) of third-neighbor cation-anion pairs in the unit cell. A ratio of  $N_{\text{third}}$  and  $p$  corresponds to hexagonality. The  $p$  is the number of cation-anion bilayers in the unit cell. In our previous study,<sup>12–14</sup> we determined this relation up to 12H. In 2H~6H-BN(AlN)<sup>12</sup> and 10H-BN(AlN)<sup>13</sup> and 12H-BN,<sup>14</sup> the total energy increases (decreases) with increasing hexagonality.

The other purpose of this study is to investigate the order of the total energies in different 30H-BN polytype structures. As for BN, there are no studies to investigate the relationship between the total energy and hexagonality in the 30H polytype. It is necessary to clarify whether the relation of the total energy and hexagonality in the 30H polytype is invariant or not on the comparison of the previous results.<sup>12–14</sup> It is expected that 30H-BN(ABC—ACB) is energetically more favorable than 30H-BN(ABC—BCB) due to lower hexagonality of the former structure. Their electronic and energetic properties of calculated two 30H-BN polytype structures have been definitively established in this study although the 30H polytype has quite huge number of possible structures (over 6000000).

## 2. Method of Calculation

The present calculation is based on the local density approximation (LDA) in density functional theory<sup>16,17</sup> (DFT) with the von-Barth and Hedin (BH) interpolation formula<sup>18</sup> for the exchange-correlation. The optimized pseudopotentials by Troullier and Martins (TM)<sup>19,20</sup> are used for B and N. Nonlocal parts of the pseudopotentials are transformed to the Kleinman-Bylander separable forms<sup>21</sup> without ghost bands. Mesh sizes of sampling  $k$ -points in an irreducible Brillouin zone (IBZ) for the 30H polytype structures are  $12 \times 12 \times 8$ ,  $12 \times 12 \times 2$ , and  $6 \times 6 \times 2$ . A smaller mesh as  $2 \times 2 \times 1$  in the whole Brillouin zone (WBZ) is used in order to compare with the results in the denser mesh. The denser mesh as  $18 \times 18 \times 12$  is used for 6H-BN. A convergence of lattice parameters is sufficient at the  $12 \times 12 \times 2$  mesh because all calculated polytypes are non-metallic and lattice constant  $c$  is quite large in the 30H polytype. The total energy difference between  $12 \times 12 \times 2$  and  $6 \times 6 \times 2$  is approximately 4 meV/B<sub>2</sub>N<sub>2</sub> = 1 meV/one atom in 30H-BN(ABC—ACB). The total energy difference between  $18 \times 18 \times 12$  and  $12 \times 12 \times 8$  is approximately 1 meV/B<sub>2</sub>N<sub>2</sub> in 6H-BN. Therefore, the structural optimization using the total energy pseudopotential method is performed up to the  $12 \times 12 \times 2$  mesh.

$12 \times 12 \times 8$  for 30H-BN and  $18 \times 18 \times 12$  for 6H-BN are used in order to obtain more detailed electronic properties (VBM, CBM, and electronic band structures).

The wave function is expanded in plane waves and the cutoff energy is 144 Ry in all calculated structures. The number of plane waves is about 68000. As for the cutoff energy, a sufficient convergence in hexagonal-BN ( $h$ -BN) was obtained at 144 Ry in the previous study.<sup>22</sup> A structural optimization of internal and cell parameters was performed using Hellmann-Feynman forces and stresses<sup>23</sup> in the unit cell, respectively. Our criterion for optimizing the internal coordinates is that the maximum force acting on each atom should be less than  $5.0 \times 10^{-4}$  Ry/Bohr, and that for optimizing the unit cell surfaces is that the maximum stress acting on each unit cell surface should be less than 0.03 GPa.

The number of atoms ( $N_{\text{atom}}$ ) in the unit cell is 60 in the 30H polytype. All possible hexagonalities in the 30H polytype are not considered due to limitations on computer resources in this study. Calculated two structures in the 30H-BN polytype are shown in Fig. 2 and Fig. 3. The number of atoms/layers ( $N_{\text{atom}}/N_{\text{layer}}$ ) and structural symmetries for 2H~6H,<sup>12</sup> and calculated 10H, 12H,<sup>13,14</sup> and 30H polytypes are tabulated in Table 1.

## 3. Results and Discussion

### 3.1 Lattice properties

The optimized lattice properties and hexagonalities (%) of the 30H-BN polytype structures are tabulated in Table 2. Experimental lattice properties of 6H-BN,<sup>1</sup> 10H-BN<sup>24</sup> and 30H-BN<sup>1</sup> are also tabulated and they agree well with our results. We have already discussed the calculated lattice constants of 6H-BN and 10H-BN with the experimental results<sup>1,24</sup> in the previous studies.<sup>12,13</sup> From Table 2, experimental lattice constant  $a$  of 6H-BN is smaller by 0.83% and 0.71% than those of 6H-BN(ABCACB) and 6H-BN(ABCBCB), respectively. Experimental lattice constant  $c$  of 6H-BN is larger by 0.31% and smaller by 0.01% than those of 6H-BN(ABCACB) and 6H-BN(ABCBCB), respectively. Experimental lattice constant  $a$  of 30H-BN is smaller by 0.51% and 0.83% than those of 30H-BN(ABC—ACB) and 30H-BN(ABC—BCB), respectively. Experimental lattice constant  $c$  of 30H-BN is larger by 1.14% and 0.31% than those of 30H-BN(ABC—ACB) and 30H-BN(ABC—BCB), respectively. Although experimental lattice constants of 6H-BN in Table 2 are slightly different from those in the previous study,<sup>12</sup> their differences are quite small within 0.1%. In experiment, the detailed structures (ABC stacking, internal parameters, symmetries) have not been determined definitely. Differences in lattice constants  $c$  and  $a$  between calculated two 30H-BN polytype structures are small within 1.0%. Lattice constants  $a$  ( $c/p$ ) of BN polytypes decrease (increase) slightly with increasing hexagonality in Table 2. Atomic displacements of internal parameters from the ideal positions in the calculated 30H polytype structures are quite small, within approximately 0.1% of lattice constant  $c$ .

### 3.2 Total energies and stability

The total energies per B<sub>2</sub>N<sub>2</sub> in the calculated 30H-BN polytype structures are tabulated in Table 2. The previous

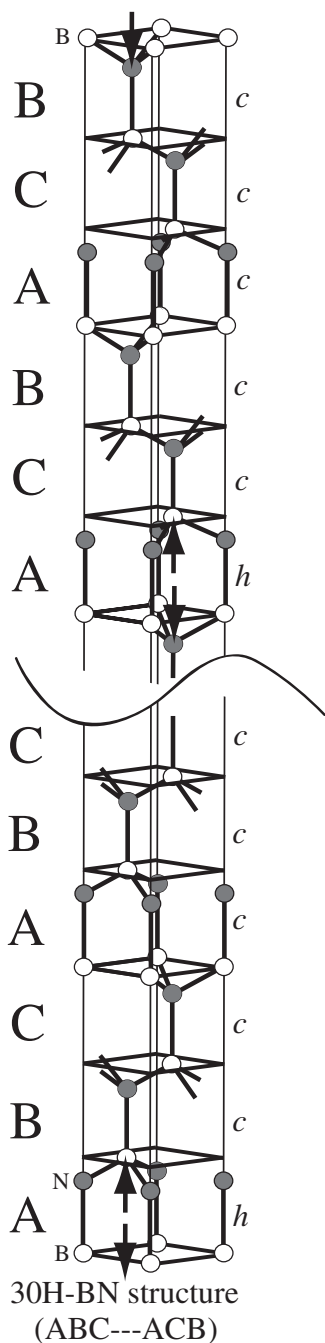


Fig. 2 The crystal structure of 30H-BN(ABC—ACB). This is shown partially because of quite large lattice constant  $c$ .

results of 2H-~6H-BN<sup>12)</sup> and 10H-BN,<sup>13)</sup> and 12H-BN<sup>14)</sup> are also tabulated in order to compare with present results. Total energy differences per  $B_2N_2$ , which are denoted by  $\Delta E$ , are also tabulated in Table 2. From Table 2, the total energy of 30H-BN(ABC—ACB) is lower than that of 30H-BN(ABC—BCB). The total energy value of 30H-BN(ABC—ACB,  $H = 6.7\%$ ) is lower than that of 12H-BN(ABCABCACBACB,  $H = 16.7\%$ ) and that of 30H-BN(ABC—BCB,  $H = 93.3\%$ ) is higher than that of 12H-BN(ABCBCBCB-ABAB,  $H = 83.3\%$ ). The polytype structure with lower hexagonality is more stable in 30H-BN although the number of calculated polytype structures in this study is two. This trend is consistent with 2H-~6H-BN,<sup>12)</sup> 10H-BN,<sup>13)</sup> and

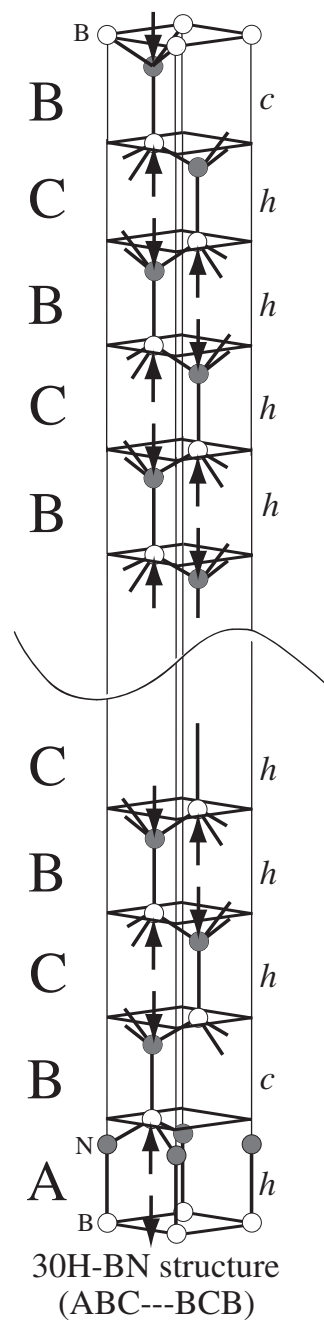


Fig. 3 The crystal structure of 30H-BN(ABC—BCB). This is shown partially because of quite large lattice constant  $c$ .

12H-BN<sup>14)</sup> in Table 2. However, the order of the total energies for calculated 30H-BN polytype structures in  $2 \times 2 \times 1$ /WBZ is opposite to the results in  $12 \times 12 \times 2$ /IBZ. Distinctly, the  $2 \times 2 \times 1$  mesh in WBZ is insufficient for accuracy.

In the BN polytype, a tetrahedral structure is formed by cation and anion atoms in the unit cell.  $c/p$  corresponds to a height of one tetrahedron in the unit cell. The  $c/p$  values of the BN polytypes increase slightly with increasing hexagonality and they are smaller at lower total energies from Table 2. Third-neighbor cation-anion atoms play a important role in the total energy lowering and stabilities in the SiC polytypes.<sup>25)</sup> The third-neighbor cation-anion pair treated in this study is the shortest of the possible third-neighbor cation-

Table 1 Symmetries of  $h$ -BN, 2H-~6H-BN, and calculated 10H-BN, 12H-BN, and 30H-BN. Calculated 30H-BN polytype structures in this study are indicated by bold letters.  $N_{\text{atom}}$  and  $N_{\text{layer}}$  are the numbers of atoms and hexagonal layers in the unit cell, respectively.  $N_{\text{third}}$  is the number of third-neighbor B-N pairs parallel to the  $c$ -axis in the unit cell.  $p$  is the number of the B-N bilayers in the unit cell. "○" indicates an existence of internal parameters. "H" indicates hexagonality (%).

	Symmetry	$N_{\text{atom}}/N_{\text{layer}}$	$N_{\text{third}}$	$p$	Internal	$H$ (%)
<b>30H-BN(ABC—ACB)</b>	$P6_3mc$	60/60	2	30	○	6.7
<b>30H-BN(ABC—BCB)</b>	$P3m1$	60/60	28	30	○	93.3
12H-BN(ABCABCACBACB)	$P6_3mc$	24/24	2	12	○	16.7
12H-BN(ABCABACABACB)	$P3m1$	24/24	4	12	○	33.3
12H-BN(ABACABCBCACB)	$P6_3mc$	24/24	6	12	○	50
12H-BN(ABCACACACACB)	$P3m1$	24/24	8	12	○	66.7
12H-BN(ABCBCBCBABAB)	$P6_3mc$	24/24	10	12	○	83.3
10H-BN(ABCABCACBACB)	$P6_3mc$	20/20	2	10	○	20
10H-BN(ABCABCABAB)	$P3m1$	20/20	4	10	○	40
10H-BN(ABCBCACBCB)	$P6_3mc$	20/20	6	10	○	60
10H-BN(ABCBCBCBCB)	$P3m1$	20/20	8	10	○	80
6H-BN(ABCACB)	$P6_3mc$	12/12	2	6	○	33
6H-BN(ABCBCB)	$P3m1$	12/12	4	6	○	66.7
5H-BN(ABCBC)	$P3m1$	10/10	2	5	○	40
4H-BN(ABCBC)	$P6_3mc$	8/8	2	4	○	50
3H-BN(ABC)	$P3m1$	6/6	0	3	○	0
2H-BN(AB)	$P6_3mc$	4/4	2	2	○	100
3C-BN	$F43m$	2/—	0	—	—	0
$h$ -BN	$P6_3/mmc$	4/2	—	—	—	—

Table 2 Optimized lattice constants  $a$  and  $c$ [nm],  $c/p$ [nm], and the  $c/a$  ratios of 30H-BN(ABC—ACB) and 30H-BN(ABC—BCB). Calculated 30H-BN polytype structures in this study are indicated by bold letters. Previous results<sup>12–14</sup> of 12H, 10H and 2H~6H polytypes are also tabulated.  $p$  is the number of B-N bilayers in the unit cell. Experimental results of 6H-BN(exp),<sup>1</sup> 10H-BN(exp)<sup>24</sup> and 30H-BN<sup>1</sup> are also tabulated.  $E_{\text{tot}}$  is the total energy per  $B_2N_2$ .  $\Delta E$  indicates the total energy difference (meV) per  $B_2N_2$  from 3C-BN. "H" indicates hexagonality (%).

	$c$	$c/p$	$a$	$c/a$	$E_{\text{tot}}$ (eV)	$\Delta E$ (meV)	$H$ (%)
2H-BN(AB)	0.4164	0.2082	0.2516	1.655	-710.54046	75	100
<b>30H-BN(ABC—BCB)</b>	6.2416	0.2081	0.2517	24.802	-710.54620	69	93.3
12H-BN(ABCBCBCBABAB)	2.4944	0.2079	0.2517	9.908	-710.55524	60	83.3
10H-BN(ABCBCBCBCB)	2.0780	0.2078	0.2518	8.253	-710.55851	57	80
12H-BN(ABCACACACACB)	2.4904	0.2075	0.2519	9.886	-710.56786	48	66.7
6H-BN(ABCBCB)	1.2451	0.2075	0.2519	4.943	-710.57003	46	66.7
10H-BN(ABACBCBCAB)	2.0742	0.2074	0.2520	8.232	-710.57400	42	60
10H-BN(ABCBCACBCB)	2.0739	0.2074	0.2520	8.231	-710.57656	39	60
12H-BN(ABACABCBCACB)	2.4862	0.2072	0.2521	9.863	-710.58289	33	50
4H-BN(ABCBC)	0.8287	0.2072	0.2521	3.288	-710.58435	31	50
10H-BN(ABCABCABAB)	2.0702	0.2070	0.2522	8.210	-710.58694	29	40
5H-BN(ABCBC)	1.0349	0.2070	0.2522	4.104	-710.58917	26	40
10H-BN(ABCACBABCBCB)	2.0699	0.2070	0.2522	8.209	-710.59127	24	40
12H-BN(ABCABACABACB)	2.4821	0.2068	0.2522	9.841	-710.59512	20.5	33.3
6H-BN(ABCACB)	1.2411	0.2069	0.2522	4.921	-710.59556	20	33.3
10H-BN(ABCABCABCBCB)	2.0659	0.2066	0.2524	8.187	-710.60316	12.5	20
10H-BN(ABCABCACBACB)	2.0659	0.2066	0.2523	8.187	-710.60365	12	20
12H-BN(ABCABCACBACB)	2.4782	0.2065	0.2524	9.819	-710.60556	10	16.7
<b>30H-BN(ABC—ACB)</b>	6.1903	0.2063	0.2525	24.516	-710.61139	4.2	6.7
3H-BN(ABC)	0.6187	0.2062	0.2526	2.449	-710.61563	0	0
3C-BN	0.3572	—	0.3572	1.000	-710.61563	0	0
30H-BN(exp <sup>1</sup> )	6.261	0.209	0.2538	24.669	—	—	—
10H-BN(exp <sup>24</sup> )	2.088	0.2088	0.2541	8.217	—	—	—
6H-BN(exp <sup>1</sup> )	1.245	0.208	0.2501	4.978	—	—	—

anion pairs. We do not consider other types of third-neighbor atoms in this study. Stability of 2H~6H polytypes for BN, SiC, and AlN has been discussed in the previous study.<sup>12)</sup> This trend for 10H-BN<sup>13)</sup> and 12H-BN<sup>14)</sup> is invariant. The third-neighbor cation-anion pairs in the calculated 6H polytype structures are indicated by arrows in Fig. 1. From Fig. 1, the third-neighbor cation-anion pair is at the hexagonal character (*h*) of the cation-anion bilayer in the unit cell. There are two third-neighbor cation-anion pairs in 6H-BN(ABCACB) and four in 6H-BN(ABCBCB). There are two third-neighbor cation-anion pairs in 30H-BN(ABC—ACB) and twenty eight in 30H-BN(ABC—BCB). These numbers ( $N_{\text{third}}$ ) are tabulated in Table 1. The ratio of  $N_{\text{third}}/p$  corresponds to hexagonality in each polytype. There is no advantage of bonding of the third-neighbor B-N atoms since covalency in the first-neighbor B-N atoms is more significant.<sup>12)</sup> The smaller bond length of the first-neighbor B-N pair is energetically more favorable in the covalent binding.  $c/p$  of the BN polytype, which is related to the bond length of the first-neighbor B-N pair, increases with increasing hexagonality. Consequently, the total energy of the BN polytype increases with increasing hexagonality.

Lattice constants  $a$  and  $c$  of 6H-BN(ABCBCB) and 30H-BN(ABC—BCB) are more agreeable with those in experiment<sup>1)</sup> than those of 6H-BN(ABCACB) and 30H-BN(ABC—ACB) although all of them agree with the experimental results within approximately 1.0%. Since the 30H polytype has over 6000000 different structures, there are many polytype structures which have the same hexagonalities of 30H-BN(ABC—ACB) and 30H-BN(ABC—BCB), respectively. Therefore, it is impossible to determine the stacking sequence of experimental 30H-BN<sup>1)</sup> definitely in this study. In contrast, the 6H-BN polytype has only two structures and their symmetries are different from each other. Thus, it may be possible to determine more easily the stacking sequence of experimental 6H-BN<sup>1)</sup> using an observation of its symmetry.

### 3.3 Electronic band structures

All calculated electronic band structures of BN polytypes in the present and previous studies are non-metallic. The hexagonal Brillouin zone is shown in Fig. 4(a) and Fig. 5(a). The electronic band structures of calculated 30H-BN polytype structures are shown in Figs. 4(b) and (c), and those of the 6H-BN polytype structures are shown in Figs. 5(b) and (c) in order to compare with the present results. In Figs. 4(b) and (c), partial bands at around the band gap in the electronic band structures are shown because there are a large number of bands in the 30H-BN polytype. All bands in the electronic structures are shown in Figs. 5(b) and (c).

Lengths of  $M$ - $L$ ,  $A$ - $\Gamma$ , and  $K$ - $H$  lines in Figs. 4(b) and (c) are quite narrow on the comparison with previous results<sup>12)</sup> because lattice constant  $c$  of the 30H polytype is quite larger than those of 2H~6H polytypes. Their lengths are expanded in order to see easily. Valence band maximum (VBM)-conduction band minimum (CBM) of BN polytypes are tabulated in Table 3. The electronic band structures of two 30H-BN polytype structures resemble each other from Figs. 4(b) and (c), although their VBM and CBM differ among them. As for 6H-BN, they have already been

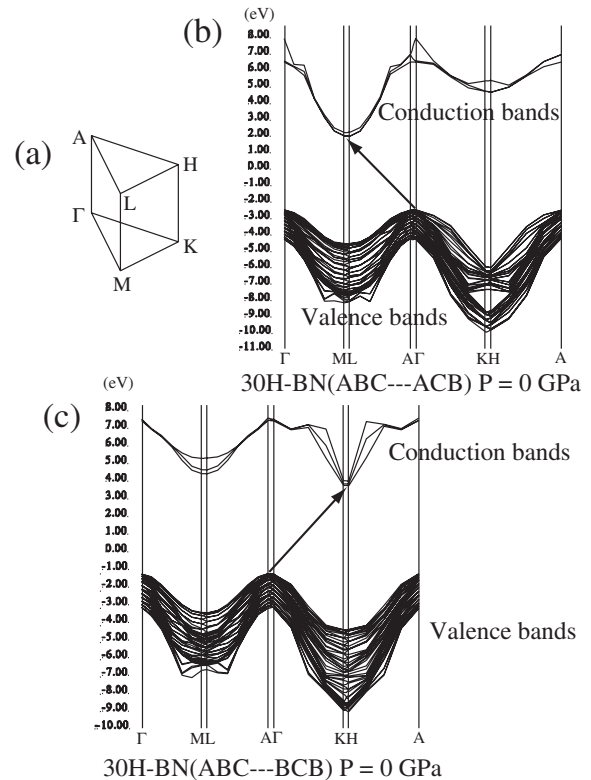


Fig. 4 Hexagonal Brillouin zone and the electronic band structures of 30H-BN(ABC—ACB) and 30H-BN(ABC—BCB). Their VBM-CBM are  $\Gamma$ - $M$  and  $A$ - $H$ , respectively. They are indicated by arrows.

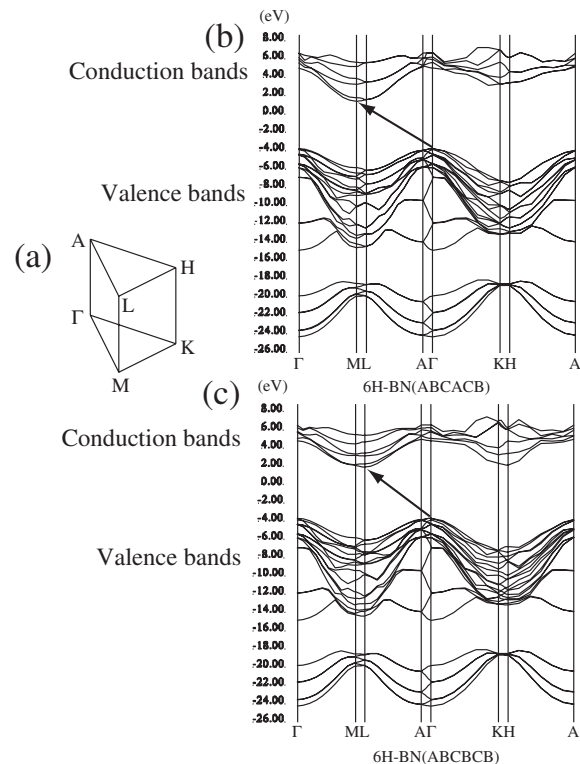


Fig. 5 Hexagonal Brillouin zone and the electronic band structures of 6H-BN(ABCACB) and 6H-BN(ABCBCB). Their VBM-CBM are  $\Gamma$ - $M$  and  $\Gamma$ - $L$ , respectively. They are indicated by arrows.

Table 3 Electronic properties of calculated 30H-BN polytype structures. Previous results<sup>12-14)</sup> of 12H, 10H and 2H~6H polytypes are also tabulated. Calculated 30H-BN polytype structures in this study are indicated by bold letters.  $\Delta_1$  and  $\Delta_2$  indicate the minimum band gap (eV) and minimum direct band gap (eV), respectively. They are underestimated in the DFT-LDA calculation. Parentheses in the  $\Delta_2$  column indicate the k-point of the minimum direct band gap. “(\*)” indicates that the k-point of the minimum direct band gap does not coincide with high symmetry k-points. “*H* (%)” indicates hexagonality (%).

		$\Delta_1$	$\Delta_2$	VBM-CBM	<i>H</i> (%)
<b>30H-BN(ABC—ACB)</b>	indirect	4.50	6.54 ( <i>M</i> )	$\Gamma$ - <i>M</i>	6.7
<b>30H-BN(ABC—BCB)</b>	indirect	4.99	7.85 ( <i>M</i> )	<i>A</i> - <i>H</i>	93.3
12H-BN(ABCABCACBACB)	indirect	4.71	6.76 ( <i>M</i> )	$\Gamma$ - <i>M</i>	16.7
12H-BN(ABCABACABACB)	indirect	4.96	7.04 ( <i>M</i> )	$\Gamma$ - <i>M</i>	33.3
12H-BN(ABACABCBCACB)	indirect	5.26	7.37 ( <i>M</i> )	$\Gamma$ - <i>M</i>	50
12H-BN(ABCACACACACB)	indirect	5.17	7.32 ( <i>M</i> )	$\Gamma$ - <i>L</i>	66.7
12H-BN(ABCBCBCBABAB)	indirect	5.48	7.87 ( <i>M</i> )	$\Gamma$ - <i>H</i>	83.3
10H-BN(ABCABCACBACB)	indirect	4.80	6.85 ( <i>M</i> )	$\Gamma$ - <i>M</i>	20
10H-BN(ABCABCACBACB)	indirect	4.62	6.68 ( <i>M</i> )	$\Gamma$ - <i>M</i>	20
10H-BN(ABCABCABAB)	indirect	4.64	6.75 ( <i>M</i> )	$\Gamma$ - <i>M</i>	40
10H-BN(ABCBCACBCB)	indirect	5.63	7.76 ( <i>M</i> )	$\Gamma$ - <i>M</i>	60
10H-BN(ABABABABAC)	indirect	5.27	7.84 ( <i>M</i> )	$\Gamma$ - <i>H</i>	80
6H-BN(ABCACB)	indirect	5.18	7.26 ( <i>M</i> )	$\Gamma$ - <i>M</i>	33.3
6H-BN(ABCBCB)	indirect	5.60	7.89 ( <i>U</i> )	$\Gamma$ - <i>L</i>	66.7
5H-BN(ABCBC)	indirect	4.93	7.02 ( <i>L</i> )	$\Gamma$ - <i>L</i>	40
4H-BN(ABCBC)	indirect	5.52	7.63 ( <i>M</i> )	$\Gamma$ - <i>M</i>	50
3H-BN(ABC)	indirect	4.43	6.94 (*)	$\Gamma$ - <i>M</i>	0
2H-BN(AB)	indirect	4.94	8.30 (*)	$\Gamma$ - <i>K</i>	100
3C-BN	indirect	4.43	8.83 ( $\Gamma$ )	$\Gamma$ - <i>X</i>	0

investigated in the previous study<sup>12)</sup> and their electronic band structures also resemble each other. Since differences of dispersion, degeneracy and splitting in most individual bands are quite small, it is impossible to discuss their stabilities from their electronic band structures. In Figs. 5(b) and (c), the denser mesh as  $18 \times 18 \times 12$  is used and the electronic properties (VBM and CBM) are invariant on the comparison of the previous results<sup>12)</sup> in  $12 \times 12 \times 8$ .

The minimum band gap ( $\Delta_1$ ) and minimum direct band gap ( $\Delta_2$ ) of BN polytypes are also tabulated in Table 3. It should be noted that these values ( $\Delta_1$ ) are underestimated in the DFT-LDA calculations. All band gaps of calculated 30H-BN polytype structures are indirect. VBM of 30H-BN(ABC—ACB) is the  $\Gamma$  point. This is a typical feature of *p*-states in *sp*<sup>3</sup>-bonded III-V and VI-VI compounds, and 2H~6H polytypes for BN, SiC, and AlN,<sup>12)</sup> 10H-BN<sup>13)</sup> and 12H-BN.<sup>14)</sup> In contrast, VBM of 30H-BN(ABC—BCB) is the *A* point where an energy difference between highest occupied bands at  $\Gamma$  and *A* is 4.1 meV. This value (4.1 meV) is small and the  $\Gamma$ -*A* line is nearly flat. Therefore, this VBM at the *A* point may be variable in more accurate calculations. It needs further consideration in the future task.

CBM of 3H-BN (*H* = 0%) is *M* and the lowest conduction band at the *M*-*L* line is lower than that at the *K*-*H* line. CBM of 30H-BN(ABC—ACB, *H* = 6.7%) is *M*. From previous studies,<sup>12,13)</sup> the energy difference between the lowest conduction bands at the *K*-*H* and *M*-*L* lines decreases with increasing hexagonality. The lowest conduction bands of the calculated BN polytypes whose hexagonalities are more than 80% at the *K*-*H* line are lower than those at the *M*-*L* line with the exception of 2H-BN (*H* = 100%). The lowest conduction band at the *H* point is higher than that at the *M*-*L* line

although that at the *K* point is lower than that at the *M*-*L* line due to the large dispersion in 2H-BN. Therefore, CBM of the BN polytypes with large hexagonality (over 80%) in Table 3 are at the *K* or *H* point although CBM of most BN polytypes are at the *M* or *L* point. CBM of 30H-BN(ABC—BCB, *H* = 93.3%) is *H* and the lowest conduction band at the *K*-*H* line is lower than that at the *M*-*L* line and CBM of 2H-BN (*H* = 100%) is *K*. A most part (93.3%) of 30H-BN(ABC—BCB) is the same stacking structure of 2H-BN. The lowest conduction band at the *K*-*H* line in 30H-BN(ABC—BCB) is nearly flat since the energy difference between the lowest conduction bands at *K* and *H* is quite small. The lowest conduction band of 30H-BN(ABC—BCB) at the *H* point is slightly lower by 5.4 meV than that at the *K* point. In contrast, the lowest conduction band of 2H-BN at the *K* point is lower by 4.6 eV than that at the *H* point and it is dispersive. It is likely that the flat band at the *K*-*H* line in 30H-BN(ABC—BCB) is originated from the folding on the *K*-*H* line due to large lattice constant *c*. The positions of CBM in SiC polytypes have been discussed<sup>26)</sup> in detail and this trend is invariant to the BN polytypes because the most VBM and CBM of the BN polytypes are equal to those of the SiC polytypes.<sup>12)</sup>

The  $\Delta_1$  values of the 3H-BN polytype (= 3C-BN) are smallest in BN polytypes from Table 3. A difference between the largest and smallest  $\Delta_1$  values are more than about 1 eV. The largest  $\Delta_1$  value in BN polytypes is 5.63 eV for 10H-BN(ABCBCACBCB, *H* = 60%). The  $\Delta_1$  value of 6H-BN(ABCBCB, *H* = 66.7%) is second largest with 5.60 eV which is slightly smaller by 0.03 eV than that of 10H-BN(ABCBCACBCB). The values of  $\Delta_1$  for 30H-BN(ABC—ACB) and 30H-BN(ABC—BCB) are 4.50 eV and 4.99 eV,

respectively. The  $\Delta_1$  values of BN polytypes whose hexagonalities are around 60% (50%~80%) may be maximum. However, the present and previous<sup>12,13</sup> results are not enough to describe it. Although the  $\Delta_1$  values are inaccurate and 6H-BN(ABCBCB) and 10H-BN(ABCBCACBCB) are not energetically favorable, a wide band gap ( $> 6$  eV) may be realized actually. As for 10H-BN(ABCBCACBCB), there are no experimental and theoretical reports with the exception of the previous studies.<sup>13,24</sup> In this study we do not treat the 30H-BN polytype structures whose hexagonalities are around 60% (50%~80%). They may have band gaps which are larger than that (5.63 eV) of 10H-BN(ABCBCACBCB).

#### 4. Summary

We have calculated the electronic and lattice properties of two 30H-BN polytype structures using the total energy pseudopotential method. Two stacking sequences as ABC—ACB and ABC—BCB in the 30H polytype were treated in this study. Their comparable lattice constants  $a$  and  $c$  agree well with the experimental results.<sup>1</sup> As a result, the total energy of calculated 30H-BN(ABC—ACB,  $H = 6.7\%$ ) is energetically more favorable than that of 30H-BN(ABC—BCB,  $H = 93.3\%$ ). In the calculated two structures of the 30H-BN polytype, covalency is dominant and this leads to stabilizing the BN polytype with smaller hexagonality. This trend is consistent with the previous results.<sup>12,13</sup> It is found that the relation of the total energy and hexagonality is invariant at least in larger stacked  $p$ H-BN polytypes ( $p = 30$ ). A clear guide is given for determining the order of stability and it is possible to predict the order of stability among possible stacking sequences in any  $p$ H-BN polytype.

We have obtained the electronic band structures, the band gap values ( $\Delta_1, \Delta_2$ ), and VBM-CBM of two 30H-BN polytype structures. The detailed electronic band structures have been clarified in this study and they are non-metallic and similar to each other. All calculated minimum band gaps are indirect in this study. VBM and CBM of 30H-BN(ABC—ACB) are  $\Gamma$  and  $M$ , respectively, and those of 30H-BN(ABC—BCB) are  $A$  and  $H$ , respectively.

Since the 30H polytype is a large system and consumes the computer resources in the total energy pseudopotential method with the structural optimization, we do not investigate all possible structures (hexagonalities) of them. From the previous studies,<sup>12,13</sup> the total energy of the AlN polytype decreases with increasing hexagonality. This trend is oppo-

site to BN polytypes. Our next task is to investigate electronic and lattice properties of 30H-AlN polytype structures in order to compare with the results of 30H-BN.

#### Acknowledgements

The numerical calculations were performed using the HP xw4400, xw4600, z400, DL160, EPSON Endeavor Pro7000 workstations, and the numerical materials simulator [Altix, SGI] in NIMS.

#### REFERENCES

- 1) S. Komatsu, K. Kobayashi, Y. Sato, D. Hirano, T. Nakamura, T. Nagata, T. Chikyo, T. Watanabe, T. Takizawa, K. Nakamura and T. Hashimoto: J. Phys. Chem. C submitted.
- 2) S. Komatsu, Y. Sato, D. Hirano, T. Nakamura, K. Koga, A. Yamamoto, T. Nagata, T. Chikyo, T. Watanabe, T. Takizawa, K. Nakamura, T. Hashimoto and M. Shiratani: J. Phys. D: Appl. Phys. **42** (2009) 225107.
- 3) A. R. Verma and P. Krishna: *Polymorphism and Polytypism in Crystals*, (Wiley, New York, 1966).
- 4) A. J. C. Wilson and E. Prince ed.: *International Table for Crystallography*, (Kluwer, Dordrecht, 2004) Vol. C, Chap. 9.2, pp. 744–765.
- 5) K. T. Park, K. Terakura and N. Hamada: J. Phys. C: Solid State Phys. **20** (1987) 1241–1251.
- 6) Y. Xu and Y. Ching: Phys. Rev. B **44** (1991) 7787–7798.
- 7) J. Furthmüller, J. Hafner and G. Kresse: Phys. Rev. B **50** (1994) 15606–15622.
- 8) A. Janotti, S.-H. Wei and D. J. Singh: Phys. Rev. B **64** (2001) 174107.
- 9) K. Shirai, H. Fujita and H. Katayama-Yoshida: phys. stat. sol. (b) **235** (2003) 526–530.
- 10) O. Mishima and K. Era: *Electric Refractory Materials*, ed. Y. Kumashiro (Marcel Dekker, New York, 2000) pp. 495–556.
- 11) K. Kobayashi and S. Komatsu: J. Phys. Soc. Jpn. **76** (2007) 113707.
- 12) K. Kobayashi and S. Komatsu: J. Phys. Soc. Jpn. **77** (2008) 084703.
- 13) K. Kobayashi and S. Komatsu: J. Phys. Soc. Jpn. **78** (2009) 044706.
- 14) K. Kobayashi: unpublished.
- 15) J. E. Iglesias: Acta Cryst. A **62** (2006) 178–194.
- 16) P. Hohenberg and W. Kohn: Phys. Rev. **136** (1964) B864–B871.
- 17) W. Kohn and L. J. Sham: Phys. Rev. **140** (1965) A1133–A1138.
- 18) U. von Barth and L. Hedin: J. Phys. C **5** (1972) 1629–1642.
- 19) N. Troullier and J. L. Martins: Phys. Rev. B **43** (1991) 1993–2006.
- 20) K. Kobayashi: Mater. Trans. **42** (2001) 2153–2156.
- 21) L. Kleinman and D. M. Bylander: Phys. Rev. Lett. **48** (1982) 1425–1428.
- 22) K. Kobayashi, K. Watanabe and T. Taniguchi: J. Phys. Soc. Jpn. **76** (2007) 104707.
- 23) O. H. Nielsen and R. M. Martin: Phys. Rev. B **32** (1985) 3792–3805.
- 24) S. Komatsu: unpublished.
- 25) C. H. Park, B. Cheong, K. Lee and K. J. Chang: Phys. Rev. B **49** (1994) 4485–4493.
- 26) P. Käckell, B. Wenzien and F. Bechstedt: Phys. Rev. B **50** (1994) 10761–10768.